WAVE-MIXING EXPERIMENTS WITH MULTI-COLOUR SEEDED FEL PULSES

F. Bencivenga#, A. Battistoni, F. Capotondi, R. Cucini, M. B. Danailov, G. De Ninno, M. Kiskinova, C. Masciovecchio, Elettra-Sincrotrone Trieste S.C.p.A., SS 14 km 163,5 in AREA Science Park, 34149 Basovizza, Trieste, Italy

Abstract

The extension of wave-mixing experiments in the extreme ultraviolet (EUV) and x-ray spectral range represents one of the major breakthroughs for ultrafast x-ray science. Essential prerequisites to develop such kind of non-linear coherent methods are the strength of the input fields, comparable with the atomic field one, as well as the high temporal coherence and stability of the photon source(s). These characteristics are easily achievable by optical lasers. Seeded free-electron-lasers (FELs) are similar in many respects to conventional lasers, hence calling for the development of wave-mixing methods. At the FERMI seeded FEL facility this ambitious task is tackled by the TIMER project, which includes the realization of a dedicated experimental end-station. The wave-mixing approach will be initially used to study collective atomic dynamics in disordered systems and nanostructures, through transient grating (TG) experiments. However, the wavelength and polarization tunability of FERMI, as well as the possibility to radiate multi-colour seeded FEL pulses, would allow to expand the range of possible scientific applications.

INTRODUCTION

Non-linear coherent methods based on wave-mixing processes are nowadays used in the optical domain to study a vast array of dynamical processes, taking place over a wide timescale range, with high time resolution as well as energy and wavevector selectivity [1]. In a typical wave-mixing experiment two or more coherent optical fields (input fields) interfere into the sample giving rise to a signal field. The large number of combinations between the parameters of the input fields (wavelength, polarization, bandwidth, arrival time, angle of incidence, etc.) allows to obtain selective information on very different dynamical processes occurring into the sample, some of them non achievable by linear methods [1].

The possibility to extend the wave-mixing approach at wavelengths shorter than the optical ones have attracted the interest of the scientific community and resulted into several theoretical and perspective works and also practical discussions on how to achieve this goal [2-5]. The only experimental report on a wave-mixing process stimulated by EUV/x-ray radiation is an optical/x-ray second order (three-wave-mixing) process, reported in [6]. More recently, we used a specially designed setup [7] to demonstrate the occurrence of a four-wave-mixing (FWM) process stimulated by the EUV coherent photon pulses radiated by FERMI [8].

Some of the major advantages in using EUV/x-ray photons with respect to optical ones are related to the possibility to: (i) achieve element selectivity through the exploitation of core resonances [2,4], (ii) probe high energy collective excitations, as valence band excitons or plasmons [2,4], (iii) exploit a much larger wavevector range, which can compare or even exceed the inverse inter-atomic/molecular distances and may thus allow for atomic/molecular-scale resolution [4,9].

WAVE-MIXING: BASIC CONCEPTS

On formal grounds, non-linear radiation-matter interactions can be described by replacing the basic relation $\mathbf{P}=\varepsilon_0\chi\cdot\mathbf{E}$ (where $\mathbf{P}$, ε_0, χ and $\mathbf{E}$ are the polarization vector, the vacuum permittivity, the linear susceptibility tensor and the electric field vector impinging into the sample, respectively) with a power expansion in $\mathbf{E}$, i.e. [1]:

$$\mathbf{P}=\mathbf{P}^{L}+\mathbf{P}^{NL}=\varepsilon_0\chi\cdot\mathbf{E}+\varepsilon_0\Sigma_{n>2}\chi^{(n)}\cdot\mathbf{E}^{n}, \quad (1)$$

where $\mathbf{P}^{L}$ and $\mathbf{P}^{NL}$ are the linear and non-linear terms of the induced polarization, while $\chi^{(n)}$ is the n^{th}-order susceptibility tensor (of rank n+1), associated to (n+1)-wave-mixing processes. When Eq. 1 is inserted into the Maxwell equations one obtains an inhomogeneous wave equation, in which each "$\chi^{(n)}\cdot\mathbf{E}_1\cdot\mathbf{E}_2\cdot\ldots\mathbf{E}_n$" term plays the role of a driving force. These can be regarded as radiation sources at frequency $\omega_{nwm,p}=\pm\omega_1\pm\omega_2\ldots\pm\omega_n$, where ω_i (i=1-n) are the frequencies of the n input fields while p labels the possible $\pm\omega_i$ permutations. It is worth noticing that $\omega_{nwm,p}$ are not necessarily equal to any ω_i.

Momentum conservation implies that the radiation emitted at $\omega_{nwm,p}$ (wave-mixing signal) is localized into a well defined region of space, centered around a $k_{nwm,p}$ vector defined by the phase matching condition: $\Delta k=|\mathbf{k}_{nwm,p}-(\pm\mathbf{k}_1\pm\mathbf{k}_2\ldots\pm\mathbf{k}_n)|=0$, where k_i (i=1-n) are the wavevectors of the input fields. In real experiments $\Delta k\neq 0$, also in light of the finite bandwidth and divergence of the input beams. However, as long as the coherence length ($L_c=\pi/\Delta k$) of the non-linear process exceeds the size of the illuminated region of the sample (L_{int}), the fields generated at different locations sample interfere constructively, leading to a N^2 increase of the non-linear signal (where N the number of elementary emitters).

#filippo.bencivenga@elettra.eu

ISBN 978-3-95450-133-5

Such a coherent addition of the non-linear emission is essential for the observation of the wave-mixing signal. Indeed, the total intensity radiated by non-linear processes is much lower than that due to linear processes. This is necessary condition to ensure the convergence of the power series shown in Eq. 1. However, since wave-mixing signals are localized in space while those arising from linear processes are much more isotropic, the latter are usually much smaller than the former in a small spatial region centered around $\mathbf{k}_{nwm}$. Other two important consequences of the phase matching constraint are: (i) $\mathbf{k}_{nwm}$ can be different from any $\mathbf{k}_i$ (see, e.g., Figs. 1c and 1e), thus largely enhancing the signal-to-noise ratio [4] and (ii) in many cases different n-wave-mixing processes cannot be simultaneously realized since their phase-matching conditions are mutually exclusive [1].

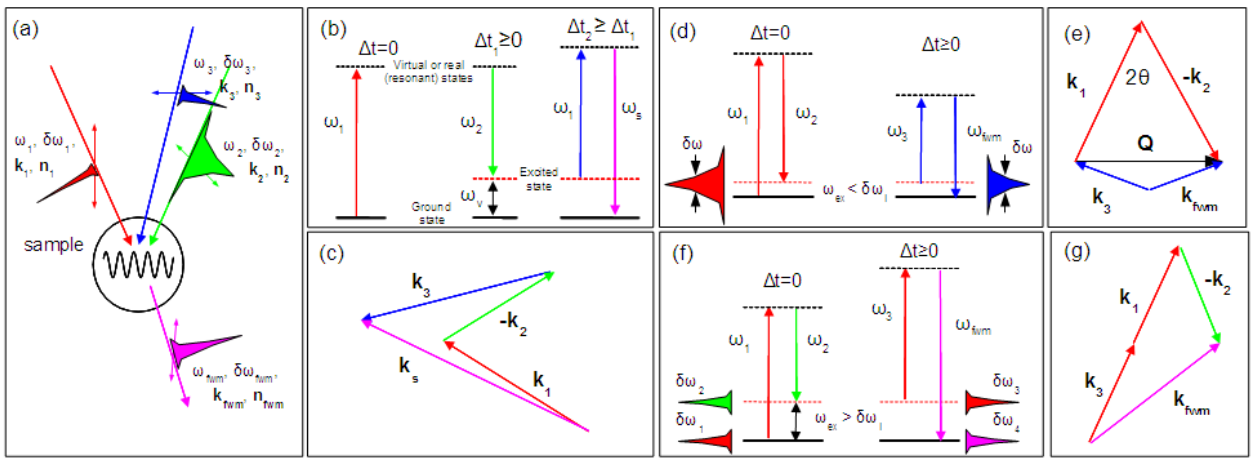

Figure 1: (a) sketch of a generic FWM experiment. ω_i, $\delta\omega_i$, $\mathbf{k}_i$ and $\mathbf{n}_i$ are the central frequency, bandwidth, wavevector and polarization of the input (i=1-3) and signal (i=fwm) fields; different colours mean different frequencies (i.e., the difference in central frequencies is larger than the bandwidth). Panels (b) and (c) are the level scheme and phase matching diagram of a generic wave-mixing experiment. Horizontal full black, dashed black and dashed red lines are the ground state, the excited state (of energy $\hbar\omega_{ex}$) and virtual or real resonant states, respectively, while Δt_1 and Δt_2 are the time delays of ω_2 and ω_3 pulses with respect to ω_1. Panels (d) and (e) are the level scheme and phase matching diagram for SBS and SRS processes; here 2θ and $\mathbf{Q}$ are the crossing angle and the excitation wavevector, respectively. (f) and (g) are, respectively, as (d) and (e) for the CARS process.

The signal intensity of a given wave-mixing process is thus related to the phase matching, usually accounted for by a $\mathrm{sinc}^2(\Delta k \cdot L_{int})$ factor, and to the magnitude of the corresponding element of the $\chi^{(n)}$ tensors. In the optical domain the latter decay as a power law of the non-linear order, i.e.: $\chi^{(n)} \sim E_a^{-(n-1)}$ [1], where $E_a = e/(4\pi\varepsilon_0 a_0^2) \sim 5 \cdot 10^{11}$ V/m (being a_0 the Bohr radius) is the atomic field strength. Furthermore, on general grounds second order processes cannot occur (i.e. $\chi^{(2)}=0$) in all centrosymmetric samples, such as liquids, glasses, polycrystalls and most of crystalline structures. In most of the cases the lowest order non-vanishing coherent non-linear interactions are hence the third order ones (i.e. FWM); second-order processes are indeed mostly used to study surfaces and interfaces, since here the inversion symmetry is broken by definition. FWM is related to the $\chi^{(3)}$ tensor and are is usually much weaker that any second order process, except the cases in which $\chi^{(2)}=0$. A typical FWM experiment is sketched in Fig. 1a-1c, while Figs. 1d-1g report the level schemes and phase matching diagrams for stimulated Brillouin/Raman scattering (SBS/SRS) and coherent antistokes Raman scattering (CARS) processes [1,10]. It is ineteresting to note how a given excitation (e.g., Raman modes in the example shown in Fig. 1) can be stimulated and probed either through SRS or CARS, depending on whenever the excitation energy ($\hbar\omega_{ex}$) is within the pulse bandwidth of the input fields or not.

Generally, the values of $\chi^{(3)}$ are expected to substantially decrease on increasing the input field frequency [1-4,11]. However, if some of the input frequencies are close to core atomic resonances, the $\chi^{(3)}$ values may be similar to (or just a few orders of magnitude lower than) those found in the optical regime [1-4,11]. On the other hand, we stress that the use of input field strength ($|\mathbf{E}_i|$) comparable or larger than E_a to compensate for the drop in the $\chi^{(3)}$ values is questionable, at least as far as one is going to use wave-mixing methods to study samples under well defined conditions. Indeed, high-field processes (as, e.g., ionization potential depression [1]) might hamper the possibility to probe the dynamics of samples in well defined thermodynamic equilibrium states.

According to [2-4,11] we have estimated a significant drop in the overall efficiency of the FWM process on going from the EUV to the x-ray regime. On such grounds we cannot exclude that in the x-ray region the signal from most of FWM processes can be appreciated and/or be hidden by that due to linear processes [4].

EUV TRANSIENT GRATING

In transient grating (TG) experiments the interference between the two equal-frequency input fileds ($\omega_1=\omega_2$)

ISBN 978-3-95450-133-5

impinges into the sample in time coincidence conditions and with a finite crossing angle (2θ); see also Figs. 1d-1e. The intereference beween these two pulses induces a transient standing electromagnetic wave with wavevector $\mathbf{Q}=\mathbf{k}_1-\mathbf{k}_2$ ($Q=|\mathbf{Q}|=4\pi \sin(2\theta/2)/\lambda_1$), which imposes a given modulation of many sample parameters, such as density, temperature or excited state populations [10]. All the excitations that may be stimulated in TG experiments are thus characterized by the same spatial periodicity, i.e. by the same Q-value. The latter can be experimentally set by 2θ and λ_1. Such a Q-selection rule allows to select a given excitation out of the Q-dispersion relations of collective modes (phonons, spin waves, polarons, etc.) or a given Q-component in the Fourier spectrum of diffusion and/or relaxation processes.

The main aim of the TIMER project is to develop EUV/soft x-ray TG methods to study the aforementioned dynamical processes through SBS and SRS experiments in the Q=0.1-1 nm^{-1} range (extendable up to Q~2-3 nm^{-1} in the near future) [9]. Such a "mesoscopic" Q-range is of the highest relevance for the study of collective atomic dynamics in disordered systems, such as glasses or liquids, as well as in systems, as gels or nanostructures, characterized by spatial periodicity or pseudo-periodicity in the ~1-100 nm range. To date, the 0.1-1 nm^{-1} Q-range is inaccessible by optical methods based on table-top or synchrotron sources [12], that are limited to $Q < 0.1$ nm^{-1}. Conversely, x-ray and thermal neutron spectroscopy cannot (with the required energy resolution) Q-values lower than ~1-2 nm^{-1}.

These experiments will be mainly carried out at the EIS-TIMER end-station [9], which is featured by an all-reflective split-delay-and-recombination system [13]. This system will be able to control both the crossing angles and arrival times of the three FEL pulses impinging into the sample. TG experiments at EIS-TIMER can also exploit the wavelength/polarization tunability of FERMI [14] and the "jitter-free" FEL/optical pump-probe system available at the facility [15]. Recently, we used the latter system and a specially designed setup to carry out FEL-based TG experiments, that demonstrated the occurrence of appreciable SBS/SRS processes stimulated by EUV radiation [8]. The experimental setup to split and recombine the FEL pulse with a finite crossing angle (2θ) is sketched in Fig. 2b and will be described in details elsewhere [7]; an image of the FEL-induced FWM signal is shown in Fig. 2c. Our setup was placed inside the DiProI experimental end-station [16], downstream an adaptive KB mirror system. The system is based on three carbon coated EUV mirrors of 70 mm length, mounted on translational and tip-tilt stages. These permit to independently vary 2θ and the time delay between the two FEL pulses ($\Delta t_{F\text{-}F}$) in the 2°-9° and -1 ps + 1 ps range, respectively; see Figs. 2d-2e. An optical setup, external to the experimental chamber, allows to use an ultrafast "jitter-free" optical pulse [15] as third input beam for FWM experiments (TG in Ref. [8]). The arrival time (Δt) and crossing angle (θ_c) of such pulse with respect to the FEL one labeled as FEL_A in Fig. 2b can be varied in the -10 ps +200 ps and 43°-47° range, respectively. The external laser was also used to calibrate $\Delta t_{F\text{-}F}$ vs d1/d2 (see Fig. 2e) through FEL-pump/optical-probe transient reflectivity measurements. The main limitation of our setup is the maximum Q-value, which is limited to $Q < 0.04$ nm^{-1} (i.e. below the "mesoscopic" range of interest) by the wavelength (> 230 nm) of the optical pulse involved in the FWM process.

We finally note that the present setup could be alternatively used as a compact "split-and-delay" stage for FEL-pump/FEL-probe experiments. In this case the main advantage of our setup is the possibility to have a finite crossing angle between pump and probe pulses, thus allowing for a spatial discrimination between pump and probe pulses downstream the sample.

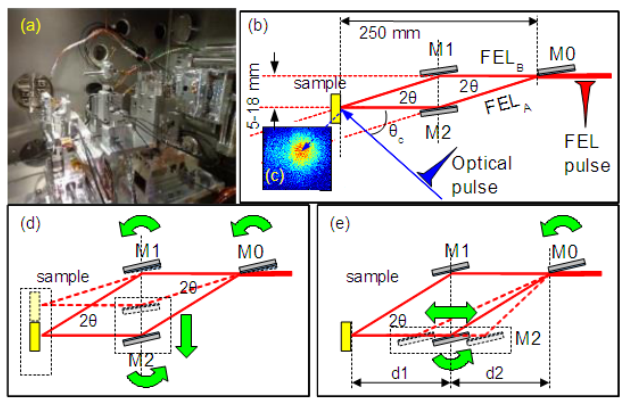

Figure 2: (a) picture of the experimental setup placed inside the DiProI experimental end station. (b) Sketch of the experimental setup: M0, M1 and M2 are C-coated plane mirrors; the relevant distances are indicated. (c) CCD image of the FWM beam. Panels (d) and (e) show how to vary 2θ and $\Delta t_{F\text{-}F}$ independently (green arrows are the involved degrees of freedom for the three mirrors), the latter task is achieved by changing the ratio d1/d2.

MULTI-COLOUR WAVE-MIXING EXPERIMENTS

The two-colour (easily upgradable at three-colour) seeded FEL emission demonstrated at FERMI [17] can be used to further develop EUV/soft x-ray TG experiments. In particular, our setup in combination with the two-colours emission in principle allows for EUV/soft x-ray coherent Raman scattering (CRS) experiments, like the ones based on the CARS process. A possible experiment of such kind was discussed in [11] and shown in Fig. 3. In this case the interference between the crossed FEL pulses (of frequency ω_1 and ω_2) gives rise to a transient grating with 'beatings' at $|\omega_1-\omega_2|$. The latter may stimulate excitations with energy ($\hbar\omega_{ex}$) exceeding the pulse bandwidth ($\hbar\delta\omega$), in contrast to TG experiments discussed in the previous section, in which $\omega_1=\omega_2$. Furthermore, since the crossing angle and the photon energy difference can be independently set, it is possible to simultaneously achieve both **Q** and ω_{ex} selectivity.

ISBN 978-3-95450-133-5

More generally, in optical CRS ω_{ex} is limited to the sub-eV range, typical of vibrational modes and low-energy electronic excitations, by the low optical photon energy (< 4-5 eV). Conversely, the much larger ω_i-values of EUV/soft x-ray photons permits to probe ω_{ex}-values of several eV's, thus allowing to study ultrafast dynamics of high-energy excitations, as valence excitons. Moreover, since the FEL-based CARS experiment shown in Fig. 3 does not involve optical pulses, the wavevector $Q=|\mathbf{k}_1-\mathbf{k}_2|$ of the probed excitation is not limited to the sub-0.1 nm^{-1} range by the (long) optical wavelength. This allows to probe dynamics at Q's comparable with the inverse molecular dimensions and intermolecular separations, and thus to gain molecular-scale spatial resolution [2]. Finally, in EUV/x-ray CRS atomic selectivity can be attained by tuning some ω_i-values to atomic resonances [2,4,11]. In these cases the high-energy (resonant) states shown in Figs. 1b, 1d and 1f correspond to real core transitions of selected elements within the sample. In light of the localization of core shells, the resonant FWM signal carry out information on the coherences between resonant atomic sites [2] and might be used, e.g., to study ultrafast charge and energy transfer processes between different atoms in molecular solids [4].

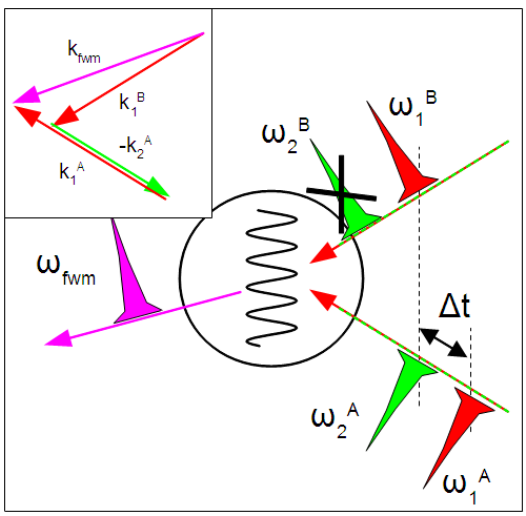

Figure 3: (main panel) sketch of a CRS experiment that may be performed at the FERMI facility exploiting the two-colour seeded FEL emission. The suffixes "A" and "B" correspond to the beam paths labelled in Fig. 1b as FEL_A and FEL_B, respectively. The crossed pulse (ω_1^B) is not involved in the FWM process. The phase matching geometry is shown in the inset.

The two-colour emission reported in [17] does not allow for $|\omega_1-\omega_2|$ values much larger than 1 eV, similarly to optical CRS, still with the possibility to exploit atomic selectivity in the excitation or probing process, not both [11]. This definitely calls for the development of novel multi-colours seeded FEL emission schemes, as these can substantially enhance the potentiality of wave-mixing experiments.

CONCLUSIONS

We reported on the development of EUV/soft x-ray wave-mixing methods at FERMI. In this context we obtained two relevant experimental results, i.e.: the demonstration of FEL-stimulated FWM processes [8] and a reliable multi-colour seeded FEL emission [17]. The combination of these two achievements opens up the possibility for a broad range of FWM applications, ranging from phonon spectroscopy to the study of low-energy coherent electronic excitations.

In the near future such studies will be carried out a more systematic way at the EIS-TIMER beamline [9]. However, it is worth mentioning that in a short term perspective FWM experiments can be in principle carried out at the DiProI end-station exploiting a specially designed setup [8].

ACKNOWLEDGEMENT

The authors acknowledge support from the European Research Council through the grant N. 202804-TIMER, the Italian Ministry of University and Research through grants FIRB-RBAP045JF2 and FIRB-RBAP06AWK3 and the Regional Government of Friuli Venezia Giulia through grant Nanotox 0060-2009.

REFERENCES

[1] R. Boyd, *Non linear optics* (Oxford: Elsevier, 2008).
[2] S. Tanaka and S. Mukamel, "Probing Exciton Dynamics Using Raman Resonances in Femtosecond X-Ray Four Wave Mixing", Phys. Rev. A 67, 033818 (2003); "Coherent X-Ray Raman Spectroscopy: A Nonlinear Local Probe for Electronic Excitations", Phys. Rev. Lett. 89, 043001 (2002); "X-ray four-wave mixing in molecules", J. Chem. Phys. 116, 1877 (2002).
[3] B. D. Patterson, "Resource Letter on Stimulated Inelastic X-ray Scattering at an XFEL", SLAC Technical Note, SLAC-TN-10-026 (2010).
[4] F. Bencivenga et al., "Nanoscale dynamics by short-wavelength four wave mixing experiments", New J. Phys. 15, 123023 (2013).
[5] G. Marcus, G. Penn, and A. A. Zholents, "Free-Electron Laser Design for Four-Wave Mixing Experiments with Soft-X-Ray Pulses", Phys. Rev. Lett. 113, 024801 (2014).
[6] T. E. Glover et al., "X-ray and optical wave mixing", Nature 488, 603 (2012).
[7] F. Capotondi et al., in preparation.
[8] F. Bencivenga et al., in preparation.
[9] F. Bencivenga and C. Masciovecchio, "FEL-based transient grating spectroscopy to investigate nanoscale dynamics", Nucl. Instrum. and Meth. A 606, 785 (2009).
[10] L. Dhar, J. A. Rogers and K. A. Nelson, "Time-resolved vibrational spectroscopy in the impulsive limit" , Chem. Rev. 94, 157 (1994).

ISBN 978-3-95450-133-5

[11] F. Bencivenga et al., "Multi-colour pulses from seeded free-electron-lasers: towards the development of non-linear core-level coherent spectroscopies", Faraday Discuss. DOI: 10.1039/c4fd00100a (2014)
[12] C. Masciovecchio, F. Bencivenga and A. Gessini, "Water dynamics at the nanoscale", Cond. Matt. Phys. 11, 47 (2008).
[13] R. Cucini, F. Bencivenga and C. Masciovecchio, "All-reflective femtosecond optical pump–probe setup for transient grating spectroscopy", Opt. Lett. 36, 1032 (2011).
[14] R. Cucini at al., "Determination of dynamical parameters in liquids by homodyne transient grating spectroscopy at large angles", Opt. Lett. 39, 5110 (2014).
[15] M. B. Danailov et al., "Towards jitter-free pump-probe measurements at seeded free electron laser facilities", Opt. Express 22, 12869 (2014).
[16] F. Capotondi et al., "Coherent imaging using seeded free-electron laser pulses with variable polarization: First results and research opportunities", Rev. Sci. Instrum. 84, 5 (2013).
[17] E. Allaria et al., "Two-colour pump–probe experiments with a twin-pulse-seed extreme ultraviolet free-electron-laser", Nat. Commun. 4, 2476 (2013).

ISBN 978-3-95450-133-5